BARC/2015/E/012

BARC/2015/E/012

भारत सरकार
Government of India

BARC REPORT

EXTERNAL

DEVELOPMENT OF INTERFACE CURRENT METHOD BASED ON 2D COLLISION PROBABILITY FOR 2D HEXAGONAL GEOMETRY

by
Suhail Ahmad Khan
Reactor Projects Division
and
Arvind Mathur
Indian Institute of Technology, Bombay, Mumbai
and
V. Jagannathan
Light Water Reactor Physics Section,
Reactor Physics Design Division *(Retired)*.

भाभा परमाणु अनुसंधान केंद्र
Bhabha Atomic Research Centre
मुंबई Mumbai - 400 085, भारत India
2015

BARC/2015/E/012

BARC/2015/E/012

GOVERNMENT OF INDIA
ATOMIC ENERGY COMMISSION

DEVELOPMENT OF INTERFACE CURRENT METHOD BASED ON 2D COLLISION PROBABILITY FOR 2D HEXAGONAL GEOMETRY

by
Suhail Ahmad Khan
Reactor Projects Division
and
Arvind Mathur
Indian Institute of Technology, Bombay, Mumbai
and
V. Jagannathan
Light Water Reactor Physics Section,
Reactor Physics Design Division *(Retired)*.

BHABHA ATOMIC RESEARCH CENTRE
MUMBAI, INDIA
2015

BIBLIOGRAPHIC DESCRIPTION SHEET FOR TECHNICAL REPORT
(as per IS : 9400 - 1980)

01	*Security classification :*	Unclassified
02	*Distribution :*	External
03	*Report status :*	New
04	*Series :*	BARC External
05	*Report type :*	Technical Report
06	*Report No. :*	BARC/2015/E/012
07	*Part No. or Volume No. :*	
08	*Contract No. :*	
10	*Title and subtitle :*	Development of interface current method based on 2D collision probability for 2D hexagonal geometry
11	*Collation :*	34p., 14 figs., 3 tabs., 1 ill.
13	*Project No. :*	
20	*Personal author(s) :*	1. Suhail Ahmad Khan 2. Arvind Mathur 3. V. Jagannathan
21	*Affiliation of author(s) :*	1. Reactor Projects Division, Bhabha Atomic Research Centre, Mumbai 2. Indian Institute of Technology, Mumbai 3. Light Water Reactor Physics Section, Reactor Physics Design Division, Bhabha Atomic Research Centre, Mumbai
22	Corporate author(s):	Bhabha Atomic Research Centre, Mumbai - 400 085
23	*Originating unit :*	Reactor Projects Division, Bhabha Atomic Research Centre, Mumbai
24	*Sponsor(s) Name :* *Type :*	Department of Atomic Energy Government

Contd...

30	*Date of submission :*	Jun 2015
31	*Publication/Issue date :*	July 2015
40	*Publisher/Distributor :*	Head, Scientific Information Resource Division, Bhabha Atomic Research Centre, Mumbai
42	*Form of distribution :*	Hard copy
50	*Language of text :*	English
51	*Language of summary :*	English
52	*No. of references :*	20 refs.
53	*Gives data on :*	

60 *Abstract :* A comprehensive code system VISWAM for physics analysis of current and future power reactors is being developed. The lattice analysis module of VISWAM code system can analyze fuel assembly (FA) cells in hexagonal, square or ring cluster geometry. The lattice analysis method initially incorporated in VISWAM code for fuel assembly (FA) analysis is based on a combination of 1D multigroup transport and a 2D few group diffusion theory. The FA consists normally of a number of heterogeneities like water pins, strong absorber pins like Gd and control absorber pins. There is a strong flux gradient between such heterogeneities and neighbouring pins which is not accurately predicted using diffusion theory. To improve this, an advanced lattice analysis method has been incorporated in VISWAM code system in hexagonal geometry. The new method is the interface current method based on 2D collision probability (CP). In this method, we have used the 2D CP method at individual lattice cells level and different lattice cells are linked using interface currents with double P2 (DP2) expansion of angular flux at cell boundaries. The FA cell in hexagonal geometry with irregular lattice structure at boundaries is modeled exactly. In this report we present the analysis of a heterogeneous benchmark problem that is typical of a high temperature test reactor (HTTR). The present report describes in detail the advanced methodology incorporated in VISWAM and the comparison of results for the HTTR benchmark with published results.

70	*Keywords/Descriptors :* HTTR REACTOR; TRANSPORT THEORY; COLLISION PROBABILITY METHOD; FUEL ASSEMBLIES; REACTOR LATTICE PARAMETERS	
71	*INIS Subject Category :*	S21
99	*Supplementary elements :*	

Development of Interface current Method based on 2D Collision Probability for 2D Hexagonal Geometry

Suhail Ahmad Khan[*†], Arvind Mathur[+] and V. Jagannathan[++]

*Reactor Projects Division, Bhabha Atomic Research Centre, Mumbai
[+]Indian Institute of Technology, Mumbai
[++]Light Water Reactor Physics Section, Reactor Physics Design Division *(Retired)*,
Bhabha Atomic Research Centre, Mumbai

suhailak@barc.gov.in; akmathur@iitb.ac.in; v_jagan1952@rediffmail.com
(†Corresponding Author)

ABSTRACT

A comprehensive code system VISWAM for physics analysis of current and future power reactors is being developed. The lattice analysis module of VISWAM code system can analyze fuel assembly (FA) cells in hexagonal, square or ring cluster geometry. The lattice analysis method initially incorporated in VISWAM code for fuel assembly (FA) analysis is based on a combination of 1D multigroup transport and a 2D few group diffusion theory. The FA consists normally of a number of heterogeneities like water pins, strong absorber pins like Gd and control absorber pins. There is a strong flux gradient between such heterogeneities and neighbouring pins which is not accurately predicted using diffusion theory. To improve this, an advanced lattice analysis method has been incorporated in VISWAM code system in hexagonal geometry. The new method is the interface current method based on 2D collision probability (CP). In this method, we have used the 2D CP method at individual lattice cells level and different lattice cells are linked using interface currents with double P2 (DP2) expansion of angular flux at cell boundaries. The FA cell in hexagonal geometry with irregular lattice structure at boundaries is modeled exactly. In this report we present the analysis of a heterogeneous benchmark problem that is typical of a high temperature test reactor (HTTR). The present report describes in detail the advanced methodology incorporated in VISWAM and the comparison of results for the HTTR benchmark with published results.

Key words: Integral transport theory, 2D Collision Probability, Interface current, High Temperature Test Reactor, Triangular pitch

1. INTRODUCTION

India is pursuing an active three stage nuclear power programme. The Unit-1 of the VVER-1000 MWe reactor commissioned in collaboration with Russia at Kudankulam has been operating at full power and another similar unit is in an advanced stage of commissioning. India is carrying out design of an innovative 600 MWth high temperature reactor (HTR) for commercial hydrogen production. To cater to the challenging physics design requirements of such reactors, a comprehensive code system VISWAM is being developed. The lattice burnup module of VISWAM code system has been completed [1, 2]. The lattice analysis method initially incorporated in VISWAM is based on pincell and supercell calculations by 1D multigroup collision probability (CP) method followed by 2D few group diffusion theory. The FA cell consists normally of a number of heterogeneities like water pins, strong absorber pins like Gd and control absorber pins. There is a strong flux gradient between such heterogeneities and neighbouring pins which is not accurately predicted using diffusion theory. To improve this, an advanced lattice analysis method has been incorporated in VISWAM code system. The CP method is an accurate and versatile method which exists in most of the popular lattice analysis codes. We have implemented the interface current method based on 2D collision probability (CP) in VISWAM code system in hexagonal geometry. In this method, the geometry of the hexagonal lattice cell is not distorted, i.e., the thin water slots at the outer boundary of the VVER type FA have been accurately described. We have applied the CP method at individual lattice cells level and linked the cells using interface currents. The incoming/outgoing angular flux is expanded up to P2 Legendre expressions at each lattice cell surface. The albedo boundary condition with unit reflection coefficient is applied on each of the hexagonal surface. The double P0/P1 (DP0/DP1) Legendre expansions of angular flux had been applied in the two dimensional fuel assembly cell calculation codes such as CASMO [3], PHOENIX [4], APOLLO [5] and DRAGON [6]. Sanchez [7] and Ouisloumen et al. [8] have applied the CP method to hexagonal assemblies with DP1 expansion. The use of DP2 expansion for hexagonal geometry is not reported in literature to the best of knowledge of the authors. Carlvik's method [9] is used to calculate the collision probabilities. In this report we will first describe the collision probability method and obtain the descretized integral transport equation in Section 2. The method of calculating collision probability matrices in 2D geometries and details of the specific numerical quadrature will be described. The solution technique to solve the descretized equations will be

presented. In the present report the analysis of a heterogeneous benchmark problem proposed by Zhang et al. [10] using the interface current method in VISWAM code is presented. The brief description of the benchmark problem is presented in Section 3. Section 4 gives the discussion of results and Section 5 gives the broad conclusions.

2. THEORY

The basic approach for the treatment of the integral form of the transport equation is to eliminate the angular dependence by projecting the equation onto a set of spherical harmonics [10]. The CP method is obtained by a limited expansion of flux. The principle of interface current method is to divide the FA into small cells and use a simple model to describe the transfer between cells. Interface current method reduces the coupling of several spatial variables, thus permitting an iterative cell by cell solution. Here we have used the 2D CP method to describe transport within the cell and different cells in FA are coupled by the interface currents.

2.1 The Integral Form of Transport Equation

The integro-differential form of neutron transport equation is [12, 13]

$$\overrightarrow{\Omega}.\,\vec{\nabla}\phi\left(\vec{r},\overrightarrow{\Omega},E\right)+\ \Sigma(\vec{r},E)\phi\left(\vec{r},\overrightarrow{\Omega},E\right)=\ q\left(\vec{r},\overrightarrow{\Omega},E\right) \tag{1}$$

where the source $q\left(\vec{r},\overrightarrow{\Omega},E\right)$ is given by

$$q\left(\vec{r},\overrightarrow{\Omega},E\right)=\ \int dE'\int d\Omega'\,\Sigma_s\left(\vec{r},\overrightarrow{\Omega'}\rightarrow\overrightarrow{\Omega},E'\rightarrow E\right)\phi\left(\vec{r},\overrightarrow{\Omega'},E'\right)+\ s(\vec{r},\overrightarrow{\Omega}) \tag{2}$$

In order to simplify the discussion we will consider one group equation and omit the energy dependence. Here the streaming operator $(\overrightarrow{\Omega}.\,\vec{\nabla})$ is just directional derivative along the direction of neutron travel. If *s* is the distance travelled by neutron along direction $\overrightarrow{\Omega}$, the streaming operator can be written as directional derivative

$$\overrightarrow{\Omega}.\,\vec{\nabla}=\ \frac{d}{ds}$$

If above equation is written at $\overrightarrow{r}+s\,\overrightarrow{\Omega}$ then

$$\frac{d}{ds}\phi\left(\overrightarrow{r}+s\,\overrightarrow{\Omega},\overrightarrow{\Omega}\right)+\ \Sigma\left(\overrightarrow{r}+s\,\overrightarrow{\Omega}\right)\phi\left(\overrightarrow{r}+s\,\overrightarrow{\Omega},\overrightarrow{\Omega}\right)=\ q\left(\overrightarrow{r}+s\,\overrightarrow{\Omega},\overrightarrow{\Omega}\right) \tag{3}$$

To derive the integral transport equation, we would like to look back along the line from which neutrons are coming. We therefore define $R = -s$, from which $d/ds = -d/dR$ and equation (3) becomes

$$-\frac{d}{dR}\phi(\vec{r}-R\,\vec{\Omega},\vec{\Omega})+\Sigma(\vec{r}-R\,\vec{\Omega})\phi(\vec{r}-R\,\vec{\Omega},\vec{\Omega})=q(\vec{r}-R\,\vec{\Omega},\vec{\Omega}) \quad (4)$$

The derivative in R is removed by using the integrating factor

$$exp\left[-\int_0^R \Sigma(\vec{r}-R'\,\vec{\Omega})\,dR'\right] \quad (5)$$

which has the property

$$\frac{d}{dR}exp\left[-\int_0^R \Sigma(\vec{r}-R'\,\vec{\Omega})\,dR'\right]=-\Sigma(\vec{r}-R\,\vec{\Omega})exp\left[-\int_0^R \Sigma(\vec{r}-R'\,\vec{\Omega})\,dR'\right] \quad (6)$$

Hence multiplying equation (4) by the itegrating factor and integrating from 0 to R gives

$$\phi(\vec{r},\vec{\Omega})=\phi(\vec{r}-R\,\vec{\Omega},\vec{\Omega})exp[-\tau(\vec{r},\vec{r}-R\,\vec{\Omega})]+\int_0^R dR'\,q(\vec{r}-R'\,\vec{\Omega},\vec{\Omega})exp[-\tau(\vec{r},\vec{r}-R'\vec{\Omega})] \quad (7)$$

Where the optical path τ between $\vec{r}$ and $\vec{r}-R'\,\vec{\Omega}$ is defined as

$$\tau(\vec{r},\vec{r}-R'\vec{\Omega})=\int_0^{R'} \Sigma(\vec{r}-R''\,\vec{\Omega})\,dR'' \quad (8)$$

Equation (7) is the required form of integral transport equation. By assuming the isotropic nature of source, the angular dependence of q in above equation can also be omitted and the equation (7) takes the following form

$$\phi(\vec{r},\vec{\Omega})=\phi(\vec{r}-R\,\vec{\Omega},\vec{\Omega})exp[-\tau(\vec{r},\vec{r}-R\,\vec{\Omega})]+\frac{1}{4\pi}\int_0^R dR'\,q(\vec{r}-R'\,\vec{\Omega})exp[-\tau(\vec{r},\vec{r}-R'\vec{\Omega})] \quad (9)$$

If the medium is bound by a surface S, equation (9) can be written as

$$\phi(\vec{r},\vec{\Omega})=\phi(\vec{r_S},\vec{\Omega})e^{-\tau_S}+\frac{1}{4\pi}\int_0^{R_S} dR'\,q\left(\vec{r'}\right)e^{-\tau(R')} \quad (10)$$

where $\vec{r_S}=\vec{r}-R_S\,\vec{\Omega}$ is an arbitrary point on the line passing through $\vec{r}$ in the direction $\vec{\Omega}$ on the surface *S*, where boundary conditions will be applied and $\vec{r'}=\vec{r}-R'\vec{\Omega}$.

The equation for scalar flux is obtained by integrating equation (10) over all angles. Thus

$$\phi(\vec{r})=\int \phi(\vec{r},\vec{\Omega})\,d\vec{\Omega}=\int_S \phi(\vec{r_S},\vec{\Omega})e^{-\tau_S}\,d\vec{\Omega}+\frac{1}{4\pi}\int_V\int_0^{R_S} q\left(\vec{r'}\right)e^{-\tau(R')}\,dR'\,d\vec{\Omega} \quad (11)$$

Now we have

$$d\vec{\Omega}=\frac{(\vec{\Omega}.\hat{n})dS}{R_S^2} \text{ and } d\vec{r}=R^2dR\,d\vec{\Omega} \quad (12)$$

So above equation can be rewritten as

$$\phi(\vec{r}) = \int_S \frac{e^{-\tau_S}}{R_S^2}\left(\overrightarrow{\Omega}.\ \hat{n}_-\right)\phi_-\left(\overrightarrow{r_S},\overrightarrow{\Omega}\right)dS + \int_V \frac{e^{-\tau(R)}}{4\pi R^2} q\left(\overrightarrow{r'}\right)d\overrightarrow{r'} \tag{13}$$

where $\phi_-\left(\overrightarrow{r_S},\overrightarrow{\Omega}\right)$is the incoming angular flux at surface *S*.

The outgoing flux at surface S can be obtained from equation (10) as it is valid at any point. The outgoing flux is given by

$$\phi_+\left(\overrightarrow{r'_S},\overrightarrow{\Omega}\right) = \phi_-\left(\overrightarrow{r_S},\overrightarrow{\Omega}\right)e^{-\tau_S} + \frac{1}{4\pi}\int_0^{R_S} dR'\, q\left(\overrightarrow{r'}\right)e^{-\tau(R')} \tag{14}$$

2.2 Discretized Flux Equation

For a given incoming angular flux to region under consideration, the system of Eqs. (13) and (14) give an exact description of the flux distribution inside the region as well as the outgoing angular flux. In order to solve these equations we have to make some numerical approximations for the scalar fluxes inside the cells and for the angular fluxes leaving and entering the cell surfaces. One assumption is the flat flux approximation inside the region, i.e. scalar flux $\phi(\vec{r})$ is constant in each region of the solution domain. Also we assume that the cross sections and the source inside each region are constant. If solution domain is divided into N_V regions of volume V_i then

$$\Sigma(\vec{r}) = \Sigma_i \text{ for } r \in V_i\,,$$
$$q(\vec{r}) = q_i \text{ for } r \in V_i\,.$$

We consider the external boundary *S* to be composed of N_S surfaces of area S_α. The angular flux on these surfaces is approximated by a series expansion in terms of half-range spherical harmonics

$$\phi_\pm\left(\overrightarrow{r_S},\overrightarrow{\Omega}\right) = \frac{1}{4\pi}\sum_{\nu=0}^{N_\nu} J_\pm^\nu(\overrightarrow{r_S})\psi^\nu(\overrightarrow{\Omega},\overrightarrow{n_\pm}). \tag{15}$$

Where N_ν is the number of terms retained in the expansion, $J_\pm^\nu$ are the expansion coefficients and $\psi^\nu$are the linearly independent functions which are taken as orthonormal and satisfy the following orthonormality condition

$$\int\left(\overrightarrow{\Omega},\overrightarrow{n_\pm}\right)\psi^\nu\left(\overrightarrow{\Omega},\overrightarrow{n_\pm}\right)\psi^\nu\left(\overrightarrow{\Omega},\overrightarrow{n_\pm}\right)d\overrightarrow{\Omega} = \pi\delta_{\mu\nu} \tag{16}$$

We define the spatially averaged fluxes and partial currents as

$$\phi_j = \frac{1}{V_j}\int_{V_j}\phi(\vec{r})\,d\vec{r} \tag{15a}$$

$$J_{\alpha}^{+} = \frac{1}{S_{\alpha}} \int_{S_{\alpha}} J(\vec{r})\, dS \tag{15b}$$

Integrating equation (13) over volume V_j of j[th] zone and multiplying the result by Σ_j

$$\Sigma_j \int_{V_j} \phi(\vec{r})\, d\vec{r} = \Sigma_j \sum_{\alpha=1}^{N_S} \int_{V_j} \int_{S} \frac{e^{-\tau_S}}{R_S^2} \left(\overrightarrow{\Omega}.\, \hat{n}_-\right) \phi_-\left(\overrightarrow{r_S}, \overrightarrow{\Omega}\right) dS\, d\vec{r}$$

$$+ \Sigma_j \sum_{i=1}^{N_V} \int_{V_j} \int_{V_i} \frac{e^{-\tau(R)}}{4\pi R^2} q\left(\overrightarrow{r'}\right) d\overrightarrow{r'}\, d\vec{r} \tag{16}$$

Now using (15) in (16) and defining

$$P_{ji} = \frac{\Sigma_j}{V_i} \int_{V_j} \int_{V_i} \frac{e^{-\tau(R)}}{4\pi R^2} d\overrightarrow{r'}\, d\vec{r}\,. \tag{17a}$$

$$P_{j\alpha}^{\nu} = \frac{\Sigma_j}{S_{\alpha}} \int_{V_j} \int_{S_{\alpha}} \frac{e^{-\tau_S}}{4\pi R_S^2} \psi^{\nu}(\overrightarrow{\Omega}, \overrightarrow{n_-}) \left(\overrightarrow{\Omega}.\hat{n}_-\right) dS\, d\vec{r}\,. \tag{17b}$$

Eq. (16) becomes

$$\Sigma_j V_j \phi_j = \sum_{\alpha=1}^{N_S} \sum_{\nu=0}^{N_\nu} P_{j\alpha}^{\nu} S_{\alpha} J_{-,\alpha}^{\nu} + \sum_{i=1}^{N_V} P_{ji}\, q_i. \tag{18}$$

Here $q_i = S_i V_i + \Sigma_{si} V_i \phi_i$ is the total source in region *i*, S_i is the fission and scattering source in a group and Σ_{si} is the self scattering cross section within the group. Here P_{ji} gives the probability of a neutron emitted uniformly and isotropically in region *i* and having its first collision in region *j* and $P_{j\alpha}^{\nu}$ gives the probability of neutron entering through surface α uniformly in mode *v* and having first collision in region *j*. The expression for outgoing current is obtained by multiplying equation (14) by $\overrightarrow{\Omega}.\, \hat{n}_+ d\vec{\Omega}$ and integrating over surface. So, we get

$$\int_{S_{\alpha}} \phi_+\left(\overrightarrow{r'_S}, \overrightarrow{\Omega}\right) \overrightarrow{\Omega}.\, \hat{n}_+\, d\vec{\Omega} dS$$

$$= \sum_{\beta=1}^{N_S} \int_{S} e^{-\tau_S}\, \phi_-\left(\overrightarrow{r_S}, \overrightarrow{\Omega}\right) \overrightarrow{\Omega}.\, \hat{n}_+ d\vec{\Omega} dS + \sum_{i=1}^{N_V} \int \frac{1}{4\pi} \int_{0}^{R_S} dR'\, q\left(\overrightarrow{r'}\right) e^{-\tau(R')}\, \overrightarrow{\Omega}.\, \hat{n}_+ d\vec{\Omega} d\vec{r}\, dS$$

Now using eq. (15) and

$$R_S^2 d\vec{\Omega} = \overrightarrow{\Omega}.\, \hat{n}_- dS$$

$$R^2 d\vec{\Omega} dR = d\vec{r}$$

and defining

$$P_{\alpha i}^{\nu} = \frac{1}{V_i}\int_{S_\alpha}\int_{V_i}\frac{e^{-\tau_S}}{4\pi R^2}\psi^{\nu}(\overrightarrow{\Omega},\overrightarrow{n_+})\,\overrightarrow{\Omega}.\hat{n}_+\,d\vec{r}dS\,. \tag{19a}$$

$$P_{\alpha\beta}^{\nu\mu} = \int\int\frac{e^{-\tau_{SS'}}}{4\pi R_S^2}\psi^{\nu}\left(\overrightarrow{\Omega},\overrightarrow{n_+}\right)\psi^{\mu}\left(\overrightarrow{\Omega},\overrightarrow{n_-}\right)\overrightarrow{\Omega}.\hat{n}_+\;\overrightarrow{\Omega}.\hat{n}_-\;dS'dS\,. \tag{19b}$$

We get

$$S_\alpha J_{+,\alpha}^{\nu} = \sum_{\beta=1}^{N_S}\sum_{\mu=0}^{N_\mu}P_{\alpha\beta}^{\nu\mu}\,J_{-,\beta}^{\mu}S_\beta + \sum_{i=1}^{N_V}P_{\alpha i}^{\nu}\,q_i\,. \tag{20}$$

Here $P_{\alpha i}^{\nu}$ is the probability that neutrons emitted uniformly and isotropically in region *i* will escape through surface α in mode *ν* and $P_{\alpha\beta}^{\nu\mu}$ is the probability that neutrons entering through surface β uniformly in mode μ will be transmitted through the cell and out through surface α in mode *ν* without making a collision. It should be noted that all the probability matrices in Eqs. (17) & (19) have a physical meaning of probabilities only for $\mu,\nu = 0$. For higher values of μ & ν, they are components of probabilities and are traditionally called probabilities.

Eqs. (18) & (20) are the required discretized equations for a cell under consideration. The physical interpretation of Eq. (18) is that the two terms on the right are the contributions to the collision rate in a region of cell from the neutrons entering through all the surfaces of the cell and sources within all the regions respectively. Similarly, in Eq. (20), the two terms on right give the contribution to the outward current through a surface of cell from the inward currents from all other surfaces of the cell plus the sources within all regions of the cell. These equations get closed by the usage of a boundary condition. Here we have used the albedo boundary condition of the form [14]

$$\phi_-\left(\overrightarrow{r_S},\overrightarrow{\Omega} - 2(\overrightarrow{n_S}.\overrightarrow{\Omega})\right) = \beta\left(\overrightarrow{r_S},\overrightarrow{\Omega}\right)\phi_+\left(\overrightarrow{r_S},\overrightarrow{\Omega}\right) \tag{21}$$

where $\beta\left(\overrightarrow{r_S},\overrightarrow{\Omega}\right)$ is the reflection coefficient at the surface *S* and $\overrightarrow{\Omega} - 2(\overrightarrow{n_S}.\overrightarrow{\Omega})$ is the final direction in which neutron travels after reflection as shown in Fig. 1.

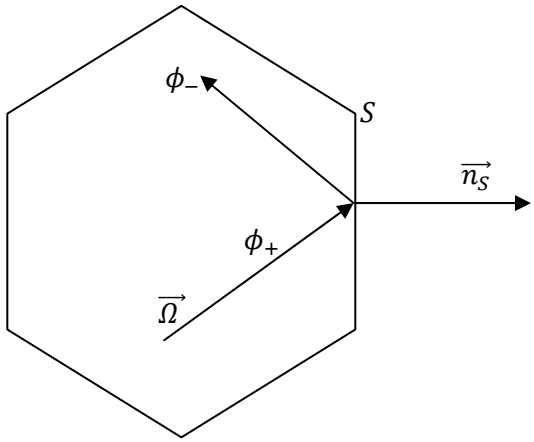

Fig. 1 Specular Reflection of neutron at the surface

The boundary condition (21), under the approximations described above, reduces to the following form

$$J^{\nu}_{-,\alpha} = \sum_{\beta=1}^{N_S} \sum_{\mu=0}^{N_\mu} A^{\nu\mu}_{\alpha\beta} J^{\mu}_{+,\beta}. \tag{22}$$

In Eq. (22) $A^{\nu\mu}_{\alpha\beta}$ is the boundary condition matrix which gives a relation between the outgoing current on a given surface and the incoming current on different surfaces.

2.3 Properties of the Collision Probability Matrices

The four types of collision probabilities defined by equations (17) and (19) satisfy some reciprocity and conservation relations. The reciprocity relations arise due to the symmetry of the optical distance i.e. $\tau\left(\overrightarrow{r},\overrightarrow{r'}\right) = \tau\left(\overrightarrow{r'},\overrightarrow{r}\right)$. We have following reciprocity relations

$$\Sigma_j V_j P_{ij} = \Sigma_i V_i P_{ji}. \tag{23a}$$

$$P^{\nu}_{i\alpha} = \frac{4\Sigma_i V_i}{S_\alpha} P^{\nu}_{\alpha i}. \tag{23b}$$

$$S_\alpha P^{\nu\mu}_{\beta\alpha} = S_\beta P^{\mu\nu}_{\alpha\beta}. \tag{23c}$$

The collision probabilities satisfy the following conservation relations

$$\sum_{j=1}^{N_V} P_{ji} + \sum_{\alpha=1}^{N_S} P^{0}_{\alpha i} = 1. \tag{24a}$$

$$\sum_{j=1}^{N_V} P^{\nu}_{j\alpha} + \sum_{\beta=1}^{N_S} P^{\nu 0}_{\beta\alpha} = \delta_{0\nu}. \tag{24b}$$

The physical interpretation of Eq. (24a) is that a neutron born in region *i* must either collide in the other regions or escape from it. Similarly for Eq. (24b), a neutron entering through a surface should either collide in one of the zones or escape through one of the surfaces.

2.4 Calculation of Collision Probabilities

The complex integrals in four types of collision probabilities given by Eqs. (17) and (19) get simplified in 2D geometry. The two dimensional space element used for calculating collision probabilities is shown in Fig. 3. We have used the following properly orthonormalized angular representation functions for DP2 expansion of angular flux [13, 15]

$$\psi^{0}_{\pm,\alpha} = 1. \tag{25a}$$

$$\psi^{1}_{\pm,\alpha} = 2\sin\vartheta\sin\phi. \tag{25b}$$

$$\psi^{2}_{\pm,\alpha} = 3\sqrt{2}(\sin\vartheta\cos\phi - \tfrac{2}{3}). \tag{25c}$$

$$\psi^{3}_{\pm,\alpha} = \tfrac{20}{\sqrt{17}}(\sin^2\vartheta - \tfrac{3}{5}\sin\vartheta\cos\phi - \tfrac{7}{20}). \tag{25d}$$

$$\psi^{4}_{\pm,\alpha} = \sqrt{306}(\sin^2\vartheta\cos^2\phi - \tfrac{2}{51}\sin^2\vartheta - \tfrac{20}{17}\sin\vartheta\cos\phi + \tfrac{16}{51}). \tag{25e}$$

$$\psi^{5}_{\pm,\alpha} = \tfrac{30}{\sqrt{11}}(\sin^2\vartheta\cos\phi\sin\phi - \tfrac{8}{15}\sin\vartheta\sin\phi). \tag{25f}$$

Where ϑ is the angle between neutron tracking direction and polar axis, and ϕ is the angle which projection of the neutron direction on 2D plane makes with the outward (+) or inward (-) normal to surface α as shown in Fig. 2. Here first function (Eq. 11a) corresponds to the P0 expansion, the first three functions (Eq. 11a to 11c) correspond to the P1 expansion and all six functions (Eq. 11) constitute the P2 expansion.

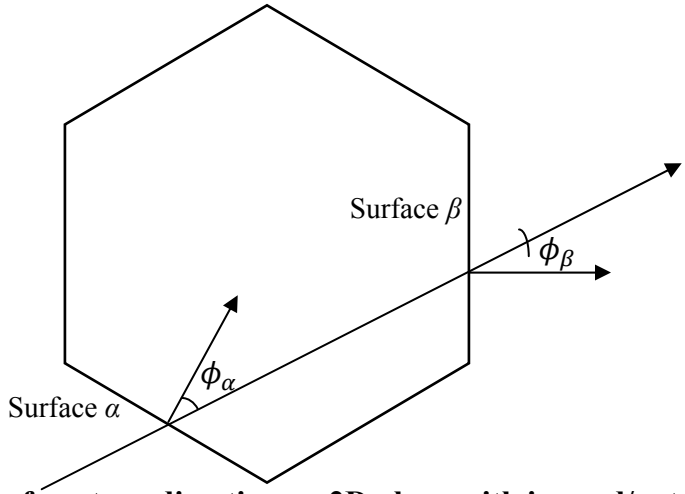

Fig. 2 Angle of projection of neutron direction on 2D plane with inward/outward normal to lattice cell surfaces

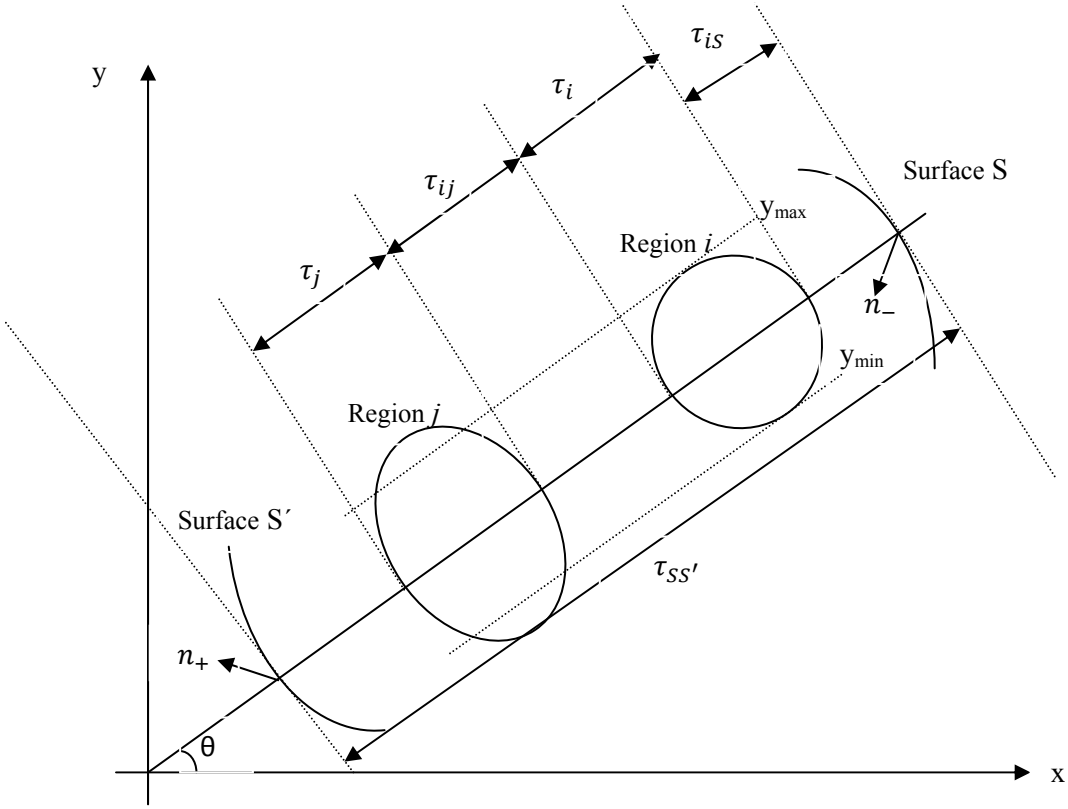

Fig. 3 Definition of two dimensional Space element

2.4.1 Region to Region Collision Probabilities

The calculation of collision probability is described in detail in references [14] & [16]. For completeness, we give here the final expressions. The region to region collision probability is given by

$$P_{ij} = \frac{1}{2\pi\Sigma_j V_j}\int_0^{2\pi}\int_{y_{min}}^{y_{max}} \left[Ki_3(\tau_{ij}) - Ki_3(\tau_{ij}+\tau_j) - Ki_3(\tau_{ij}+\tau_i) + Ki_3(\tau_{ij}+\tau_j+\tau_i)\right] dy\, d\theta. \tag{26a}$$

where the optical distances τ_i , τ_j & τ_{ij} are shown in Fig. 3 and Ki_3 is the Bickley-Naylor function of third order. The general function of order 'n' is defined as

$$Ki_n(\tau) = \int_0^{\pi/2} d\theta\, sin^{n-1}\theta\, e^{-\frac{\tau}{\sin\theta}}$$

Similarly, the self collision probability P_{ii} is obtained as

$$P_{ii} = 1 - \frac{1}{2\pi\Sigma_i V_i}\int_0^{2\pi}\int_{y_{min}}^{y_{max}} [Ki_3(0) - Ki_3(\tau_i)]\, dy\, d\theta. \tag{26b}$$

Since the sources and scattering are assumed to be isotropic, the region-to-region collision probabilities have no angular dependence.

2.4.2 Region to Surface Escape Probability

The expression for escape probability from region *i* to surface α, in eq. (19a), reduces to the following form when projected on a 2D plane

$$P_{iS_\alpha}^{\nu} = \frac{1}{4\pi\Sigma_i V_i}\int d\phi \int dy \int_0^{\pi} d\theta \, sin^2\theta \, (e^{-\frac{\tau_s}{\sin\theta}} - e^{-\frac{(\tau_i+\tau_s)}{\sin\theta}}) \, \psi_\alpha^{\nu}(\vec{\Omega}.\overrightarrow{n_+}). \tag{27}$$

The different components of region to surface escape probability are obtained using expansion functions (25) in eq. (27). The expressions are given by

$$P_{\alpha i}^{0} = \frac{1}{2\pi\Sigma_i V_i}\int_0^{2\pi}\int_{y_{min}}^{y_{max}}[Ki_3(\tau_{iS}) - Ki_3(\tau_i+\tau_{iS})]dy\, d\theta. \tag{28a}$$

$$P_{iS_\alpha}^{1} = \frac{2}{2\pi\Sigma_i V_i}\int_0^{2\pi} d\theta \int_{y_{min}}^{y_{max}} \sin\phi_\alpha \, [Ki_4(\tau_s) - Ki_4(\tau_i+\tau_s)]. \tag{28b}$$

$$P_{iS_\alpha}^{2} = -2\sqrt{2}\, p_{iS_\alpha}^{0} + \frac{3\sqrt{2}}{2\pi\Sigma_i V_i}\int_0^{2\pi} d\theta \int_{y_{min}}^{y_{max}} \cos\phi_\alpha \, [Ki_4(\tau_s) - Ki_4(\tau_i+\tau_s)]. \tag{28c}$$

$$P_{iS_\alpha}^{3} = \frac{1}{\sqrt{17}}\Big[-15\, p_{iS_\alpha}^{0} - 2\sqrt{2}\, p_{iS_\alpha}^{2} + \frac{20}{2\pi\Sigma_i V_i}\int_0^{2\pi} d\theta \int_{y_{min}}^{y_{max}}[Ki_5(\tau_s) - Ki_5(\tau_i+\tau_s)]\Big]. \tag{28d}$$

$$P_{iS_\alpha}^{4} = \frac{\sqrt{306}}{51}\Big[-24\, p_{iS_\alpha}^{0} - 10\sqrt{2}\, p_{iS_\alpha}^{2} + \frac{1}{2\pi\Sigma_i V_i}\int_0^{2\pi} d\theta \int_{y_{min}}^{y_{max}}(51cos^2\phi_\alpha - 2)[Ki_5(\tau_s) - Ki_5(\tau_i+\tau_s)]\Big]. \tag{28e}$$

$$P_{iS_\alpha}^{5} = \frac{1}{\sqrt{11}}\Big[-8\, p_{iS_\alpha}^{1} + \frac{30}{2\pi\Sigma_i V_i}\int_0^{2\pi} d\theta \int_{y_{min}}^{y_{max}} \cos\phi_\alpha \, \sin\phi_\alpha [Ki_5(\tau_s) - Ki_5(\tau_i+\tau_s)]\Big]. \tag{28f}$$

Here not all the directions of θ and intervals of y contribute to the integration. The integration over θ is limited to those directions which pass through surface α.

2.4.3 Surface to Region Probability

The zeroth component of surface to region collision probability is given by

$$P_{i\alpha}^{0} = \frac{2}{\pi S_\alpha}\int_0^{2\pi}\int_{y_{min}}^{y_{max}}[Ki_3(\tau_{iS}) - Ki_3(\tau_i+\tau_{iS})]dy\, d\theta. \tag{29}$$

The surface to region probabilities are normally not computed by direct numerical integration to save computational efforts. Reciprocity relation (23b) is utilized to directly calculate these probabilities from escape probability.

2.4.4 Surface to Surface Transmission Probability

The general formula for transmission probability from surface β to surface α, in eq. (8d), is written as follows in 2D geometry

$$p_{\alpha\beta}^{\nu\mu} = \frac{1}{\pi S_\alpha} \int d\phi \int dy \int_0^\pi d\theta \, sin^2\theta \, e^{-\frac{\tau}{\sin\theta}} \psi_\beta^\mu \left(\vec{\Omega}.\overrightarrow{n_-}\right) \psi_\alpha^\nu \left(\vec{\Omega}.\overrightarrow{n_+}\right). \tag{30}$$

The zeroth component of surface to surface transmission probability is given by

$$P_{\alpha\beta}^{00} = \frac{2}{\pi S_\beta} \int_0^{2\pi} \int_{y_{min}}^{y_{max}} Ki_3(\tau_{SS'}) dy \, d\theta. \tag{31}$$

Here too, only those y and θ intervals contribute to integration which pass through both surfaces α and β. The higher components of transmission probability are too complicated to be presented here and are obtained using higher order representation functions (25) in (30) [17].

2.5 Computation of Collision Probability Integrals

The calculation of probabilities using Eqs. (26) to (29) involves the evaluation of double integrals over y and θ numerically. These integrations are approximated by using numerical quadrature for angle and space. The problem domain is considered under different angles of rotation. For each value of θ in the quadrature, a set of parallel lines, called tracks, are drawn. We have used equidistant ray tracking method for present study. The tracking method is described in detail in Appendix A. If w_y and w_A are the weights of y and θ then

$$\int f(y,\theta) \, dy \, d\theta = \sum_p \sum_q w_{yp} w_{Aq} f(y_p, \theta_q). \tag{32}$$

For evaluating these probabilities, two types of quadrature *viz.* equiangular and Gauss-Legendre quadrature can be used for angular variable θ.

The tracking needs to be done only for a=0 to b=π, since the contribution from π to 2π will be associated with the probability p_{ji} which is symmetric to p_{ij}. If we chose N angles between 0 and π, then weights for equiangular quadrature are given by

$$w_A = \frac{(b-a)}{N} = \frac{\pi}{N}. \tag{33}$$

And the angular points are given by

$$\theta_i = \left(i - \frac{1}{2}\right) w_A = \left(i - \frac{1}{2}\right) \frac{\pi}{N} \; ; \; \forall \, i = 1, N. \tag{34}$$

The integration weights and points can also be obtained using the Gauss–Legendre quadrature. The integrations weights and points in the Gauss–Legendre quadrature are selected in such a way that:

$$\int_{-1}^{1} f(x)\, dx = \sum_{i=1}^{N} w_i\, f(x_i). \tag{35a}$$

is exact when $f(x)$ is a polynomial of order (2N-1) or lower [18]. This can be ensured by selecting x_i for each order N as the zeros of the Legendre polynomials $P_N(x)$. Once the integration points have been computed, the associated weights can be obtained using:

$$w_i = \frac{2}{(1-x_i^2)[P_N'(x_i)]^2}. \tag{35b}$$

If the limits of integration are *a* & *b,* we can use the following transformation

$$\int_{a}^{b} f(x)\, dx = \sum_{i=1}^{N} w_i'\, f(x_i'). \tag{35c}$$

such that

$$w_i' = \frac{(b-a)}{2} w_i. \tag{35d}$$

$$x_i' = \frac{(b-a)}{2} x_i + \frac{(b+a)}{2}. \tag{35e}$$

For integration limits of 0 to π, we can use Gauss–Legendre points and weights corresponding to N=2 to 20, and for 24, 28, 32, 64and 96.

For *y* integral, trapezoidal quadrature set is used. If the limits of *y* integration are from *a* to *b* and if N_y parallel lines are drawn, the separation between two lines or weight is given by

$$w_y = dy = \frac{(b-a)}{Ny}. \tag{36}$$

2.5 Normalization of Collision Probabilities

The collision probabilities calculated should satisfy the reciprocity and conservation relations given in Eqs. (23) & (24). Since we calculate the collision probabilities using numerical integrations, the conservation relations may not get satisfied due to discretizing error. The conservation relations are enforced by several normalizing schemes [13]. Here we have adopted a method proposed by Villarino *et al* [16]. In this method, we define

$$P_{ij}^{H} = (w_i + w_j)P_{ij}. \tag{37a}$$

$$P_{\alpha\beta}^{H} = (w_\alpha + w_\beta)P_{\alpha\beta} \tag{37b}$$

The conservation laws are ensured by requiring

$$\sum_a (w_a + w_b)P_{ab} = 1. \tag{38a}$$

$$\sum_a w_a P_{ab} + w_b \sum_a P_{ab} = 1. \tag{38b}$$

$$w_b = \frac{1-\sum_{a,a\neq b} w_a P_{ab}}{P_{bb}+\sum_a P_{ab}}. \tag{38c}$$

where the indices *a* and *b* run over all regions and surfaces. The Eq. (36c) is iteratively solved. Initially all the *w's* are assigned a value of 0.5, which is the value they would have if there were no errors in the probabilities. The iteration process uses an under relaxation factor of 0.7 [16]. The solution for w_a^{k+1} is assumed converged if

$$\max\left(\frac{w_a^{k+1}-w_a^k}{w_a^{k+1}}\right) \leq \epsilon. \tag{39}$$

or after a preset number of iterations, currently 20. The value used for ϵ is 10^{-5}. The advantage of this method is that by using weight factors, probabilities which are zero remain zero e.g., the self transmission probabilities $P_{\alpha\alpha}$.

To enforce the conservation relation (24b) for higher components of probabilities, we have used diagonal normalization scheme. In this scheme, the error is found using (24b) as

$$\varepsilon_\alpha^\nu = \delta_{0\nu} - \sum_{j=1}^{N_V} P_{j\alpha}^\nu - \sum_{\beta=1}^{N_S} P_{\beta\alpha}^{0\nu} \qquad \forall\, \nu > 1 \tag{40}$$

This error is adjusted in the diagonal elements of transmission probability *i.e.*

$$P_{\alpha\alpha}^\nu = P_{\alpha\alpha}^\nu + \varepsilon_\alpha^\nu. \tag{41}$$

2.6 Use of Boundary Condition and Solution of CP Equations

The multigroup transport equations to be solved in a cell containing N_V regions form a linear system. The solution method described in [19] has been adopted. In the two linear equations defined by Eqs. (18) & (20), the source q_i , written in terms of group source and self scattering source, is given by

$$q_i = \Sigma_i^s \phi_i V_i + S_i V_i. \tag{42}$$

The group source S_i is defined as

$$S_i = \left(\sum_{\substack{g'=1 \\ g' \neq g}}^{G} \Sigma_{si}^{g' \to g} \phi_i^{g'} + \frac{\chi_g}{k} \sum_{g'=1}^{G} \nu \Sigma_{fi}^{g'} \phi_i^{g'} \right). \tag{43}$$

We define the vectors for collision rate

$$\{\mathbf{f}\}_i \equiv \Sigma_i \phi_i V_i. \tag{44a}$$

the partial currents

$$\{\mathbf{j}_+\}_\alpha \equiv S_\alpha J_{+,\alpha}^{\nu}. \quad \text{and} \quad \{\mathbf{j}_-\}_\alpha \equiv S_\alpha J_{-,\alpha}^{\nu}. \tag{44b}$$

and the source

$$s_i \equiv S_i V_i. \tag{44c}$$

the source q_i given by (42) can be written in the vector form as

$$\mathbf{q} = \mathbf{C}\,\mathbf{f} + \mathbf{s}. \tag{45}$$

where **C** is a diagonal matrix defined by

$$\{\mathbf{C}\}_{ij} = \delta_{ij} \frac{\Sigma_j^s}{\Sigma_j}. \tag{46}$$

Thus Eqs. (18) & (20), can be written in the matrix for as

$$\mathbf{f} = \mathbf{P_{VV}}\,\mathbf{q} + \mathbf{P_{VS}}\,\mathbf{J}^-. \tag{47}$$

$$\mathbf{J}^+ = \mathbf{P_{SV}}\,\mathbf{q} + \mathbf{P_{SS}}\,\mathbf{J}^-. \tag{48}$$

where we have defined P_{VV} as the matrix of region to region, P_{VS} as the matrix of surface to region, P_{SV} as the matrix of region to surface and P_{SS} as the surface to surface collision probabilities respectively. The boundary condition used here is in the form of a relation between the average outgoing angular flux on surface S_β and the average incoming angular flux on a different surface S_α. In matrix form this can be written as

$$\mathbf{J}^- = \mathbf{A}\,\mathbf{J}^+. \tag{49a}$$

In the case of albedo boundary condition, the coupling boundary condition matrix can be written as

$$A_{\alpha\beta}^{\nu\mu} = \beta_\alpha \delta_{\alpha\beta} \delta^{\nu\mu}. \tag{49b}$$

where β_α is the reflection coefficient at surface α. In case of total reflection at surface α, $\beta_\alpha = 1$.

So Eq. (48) takes the form

$$\mathbf{J}^+ = (\mathbf{I} - \mathbf{A}\mathbf{P}_{\mathbf{SS}})^{-\mathbf{1}}\, \mathbf{P}_{\mathbf{SV}}\, \mathbf{q}. \tag{50}$$

Eqs. (47) & (50) are iteratively solved using the conventional inner-outer iteration scheme to calculate partial currents across the surfaces and collision rates in each region. Also a self scattering reduction scheme is adopted for eqn. (47) *i.e.* all the information of self scattering of a group is transferred to left side so that Eq. (47) takes the following form

$$\mathbf{f} = (\mathbf{I} - \mathbf{C})^{-\mathbf{1}}(\mathbf{P}_{\mathbf{VV}}\, \mathbf{s} + \mathbf{P}_{\mathbf{VS}}\, \mathbf{J}^-). \tag{51}$$

3. DESCRIPTION OF BENCHMARK

Zhang et al. [10] have proposed a simplified heterogeneous benchmark problem that is typical of a high temperature reactor. The primary aim of benchmark is to assess the accuracy of diffusion or transport methods for reactor calculations. The benchmark is derived from the experimental data of High Temperature Engineering Test Reactor (HTTR) start-up experiments, which was built by Japan in the late 1990s. The benchmark covers 2D/3D full core, single constituent fuel block of core and single pincell configurations. The present paper describes the results obtained for single pincell and single fuel block calculations. It is to be noted that the benchmark problems are heterogeneous down to the pin i.e., the coated fuel particles and the graphite matrix are homogenized and mixed into a fuel material.

The benchmark provides the six group macroscopic cross section for all the materials required as obtained by a detailed lattice calculations using HELIOS code system. Due to this no double heterogeneity treatment of TRISO fuel particle was required. The full details of benchmark can be found in [1]. Here we give only some details of fuel blocks and fuel pins analyzed. The fuel block and fuel pin, shown in Fig. 2 have a hexagonal shape. The fuel pin pitch is 5.15cm and fuel pin diameter is 4.1cm. The fuel block consists of 33 fuel pins, 3 burnable poison (BP) rods and one central graphite pin as shown in Fig. 2. The fuel block pitch is 36cm. The fuel pin and fuel block consider seven cases of fuel enrichment ranging from 3.4 to 9.9 wt%.

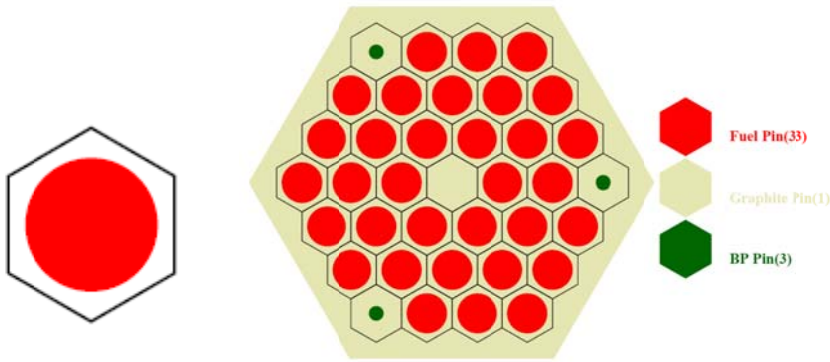

Fig. 4 – Fuel pin and Fuel Assembly Cells

3.1 Discretization of the Problem

In order to calculate multiplication factor and flux for the two problems studied, one needs to calculate the four types of CP matrices defined in (12) to (15). For pincell geometry, the mesh structure considered is shown in Fig. 5. The fuel and coolant regions were divided into finer circular regions. The fuel region was divided in three regions of equal volume and outside graphite region was divided into eight regions of equal thickness. As a result the pincell has annular shells embedded in the hexagonal geometry. Due to annular structure inside the hexagon, 1D annular treatment was done to calculate region to region collision probabilities for circular regions. Only for the outermost region 2D method was required. The albedo boundary condition with reflection coefficient of unity is used at each of the six surfaces of the hexagonal pincell.

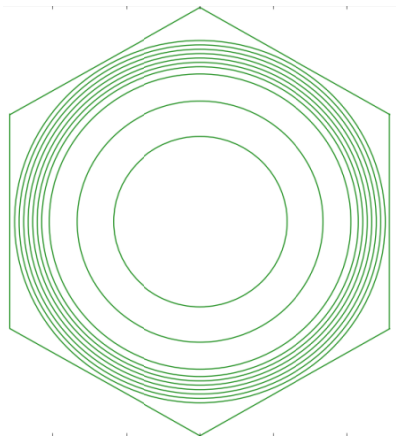

Fig. 5 – Mesh division inside single hexagonal pincell

For fuel assembly calculation, the collision probability matrices need to be calculated only for materially and geometrically distinct regions. The geometry of the hexagonal FA should be modeled exactly. As seen in Fig. 4 there is a thin layer of graphite block beyond the regular hexagonal structure in the fuel assembly. It is important to treat this region accurately. It is noted

that in some recipes this thin region is artificially expanded into full regular hexagonal structure. Any inaccurate modeling of this layer could create unwarranted errors in core calculation. To alleviate this problem in the fuel assembly cell, beyond the regular hexagonal structure, two different geometric meshes are identified which are designated as side mesh (Fig. 6a) and corner mesh (Fig. 7a). The mesh division in the regular hexagonal cells is similar to what was used for pincell calculation. The mesh division in the side and corner cells is as shown in the Figs. 6b & 7b. Within the regular hexagon structure, three distinct regions were identified *viz*. fuel pin, BP pin and graphite pin. Thus there are totally five identified distinct zones for the fuel assembly calculation. Once the CP matrices are computed for these distinct zones, the flux and multiplication factor is calculated by an iterative procedure. The boundary condition is applied at the outer boundary surfaces of side and corner meshes.

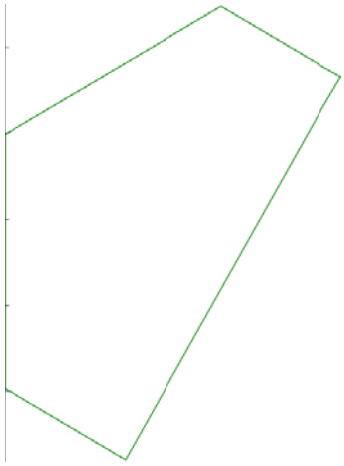

Fig. 6a – Side mesh

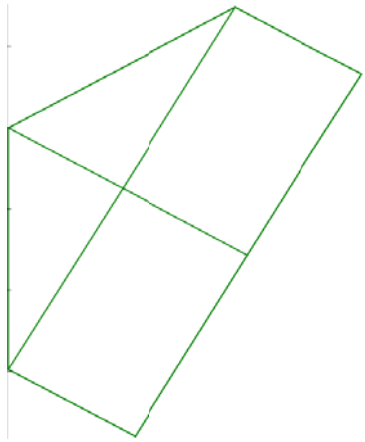

Fig. 6b – Mesh division inside Side mesh

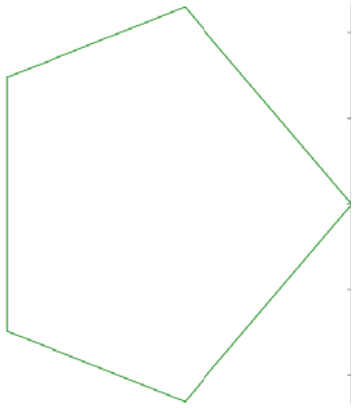

Fig. 7a – Corner mesh

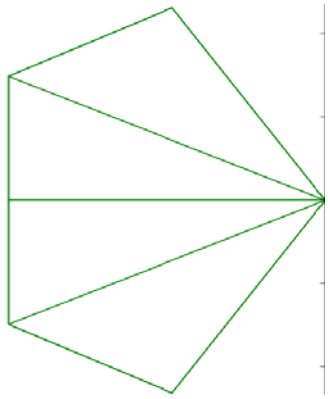

Fig. 7b – Mesh division inside Corner mesh

4. RESULTS AND DISCUSSION

The VISWAM results for single pincell and fuel block are compared with the benchmark results. The results of MOCUM code system of Yang et al. [20] are also included for comparison. MOCUM is based on the method of characteristics (MOC) and uses fine unstructured triangular meshes for discretization of the geometry. The convergence criterion for pincell calculation was taken as 10^{-9} for k_∞ and 10^{-8} for flux, whereas, for FA calculation these criterions are 10^{-7} and 10^{-6} respectively. All the VISWAM results are obtained with 32 azimuthal angles and a ray separation of 0.04cm. Table 1 gives the comparison of multiplication factor calculated with P0 model for single pincell with MOCUM & Monte Carlo results of benchmark for all seven fuel enrichments. The results show a good agreement with a maximum error of 0.01% in k_∞. Table 2 gives the comparison of k_∞ for seven fuel assembly types with P0 model in VISWAM. An error of (-0.18%) w.r.t. benchmark is obtained for first enrichment (-0.15% w.r.t. MOCUM) whereas the error for all other enrichments is within ±0.08% (±0.06% w.r.t. MOCUM). Table 3 gives the results with VISWAM k_∞ obtained using P1 and P2 expansion of angular flux. The results with P1/P2 expansion show maximum error of -0.18%/-0.17% for first enrichment. The maximum error for other enrichments is found within ±0.08% for both P1 and P2 results. In the current problem with graphite moderator there is no steep flux gradient within the fuel assembly as may be present in an assembly with light water as moderator. Therefore the use of P1 expansion is rather adequate to get the results within desirable accuracy. Use of higher order P2 expansion functions gives nearly same eigenvalue.

Tables 1 & 2 also compare the typical running time for VISWAM and MOCUM results. The VISWAM results are obtained on a windows machine equipped with 3.0GHz dual core processor and 2GB RAM. It is seen that VISWAM CPU time is significantly less compared to MOCUM but the accuracy achieved is comparable. Also it should be noted that MOCUM code is parallelized version and runs on advanced configuration machines whereas the VISWAM is running in serial mode only. It is seen from Table 3 that the DP1 and DP2 models require 8 or 13 sec compared to 5 sec of DP0 model due to the computation of extra components of CPs for higher angular flux expansion.

Fig. 8 gives the comparison of fission density distribution, obtained using P2 expansion, for first enrichment type with benchmark results. The comparison is good and shows a maximum

deviation of 0.7%. No significant differences in fission density distribution were noted with P0 and P1 expansion for first enrichment. Figs. 9 to 14 give the fission density distribution for other 4enrichment types using P0 and P2 expansion functions. This data is not available in the benchmark. Only with increasing enrichment, a small difference appears in the two fission density distributions.

Table 1 – Comparison of k_∞ for Pincell with VISWAM P0 Model

Enrichment (wt.%)	k_∞			Δk/k(%) w.r.t.		Run Time(sec)	
	VISWAM	MOCUM	Benchmark	Benchmark	MOCUM	VISWAM	MOCUM
3.4	1.13512	1.13516	1.13519	0.01	0.00	1.0	19.1
4.8	1.19575	1.19584	1.19577	0.00	0.01	1.0	14.5
5.2	1.20683	1.20694	1.20688	0.00	0.01	1.0	13.2
6.3	1.23524	1.23530	1.23531	0.01	0.01	1.0	12.0
6.7	1.24322	1.24333	1.24326	0.00	0.01	1.0	11.7
7.9	1.26042	1.26044	1.26044	0.00	0.00	1.0	10.7
9.9	1.28922	1.28926	1.28933	0.01	0.00	1.0	10.4

Table 2 – Comparison of k_∞ for Fuel Assembly with VISWAM P0 Model

Enrichment (wt.%)	k_∞			Δk/k(%) w.r.t.		Run Time	
	VISWAM	Benchmark	MOCUM	Benchmark	MOCUM	VISWAM (sec)	MOCUM (min)
3.4	1.03930	1.04119	1.04084	-0.18	-0.15	5.0	4.48
4.8	1.15214	1.15307	1.15283	-0.08	-0.06	5.0	3.76
5.2	1.17212	1.17287	1.17265	-0.06	-0.05	5.0	3.61
6.3	1.22183	1.22212	1.22192	-0.02	-0.01	5.0	3.31
6.7	1.23790	1.23802	1.23787	-0.01	0.00	5.0	3.05
7.9	1.27344	1.27323	1.27305	0.02	0.03	5.0	2.80
9.9	1.32022	1.31962	1.31951	0.05	0.05	5.0	2.40

Table 3 – Comparison of k_∞ for Fuel Assembly with higher expansion of angular flux

Enrichment (wt.%)	k_∞			Δk/k(%) w.r.t. Benchmark		VISWAM Run Time (sec)	
	VISWAM		Benchmark	DP1	DP2	DP1	DP2
	DP1	DP2					
3.4	1.03936	1.03944	1.04119	-0.18	-0.17	8.0	13.0
4.8	1.15238	1.15244	1.15307	-0.06	-0.05	8.0	13.0
5.2	1.17238	1.17245	1.17287	-0.04	-0.04	8.0	13.0
6.3	1.22217	1.22223	1.22212	0.00	0.01	8.0	13.0
6.7	1.23821	1.23826	1.23802	0.02	0.02	8.0	13.0
7.9	1.27385	1.27390	1.27323	0.05	0.05	8.0	13.0
9.9	1.32070	1.32074	1.31962	0.08	0.08	8.0	13.0

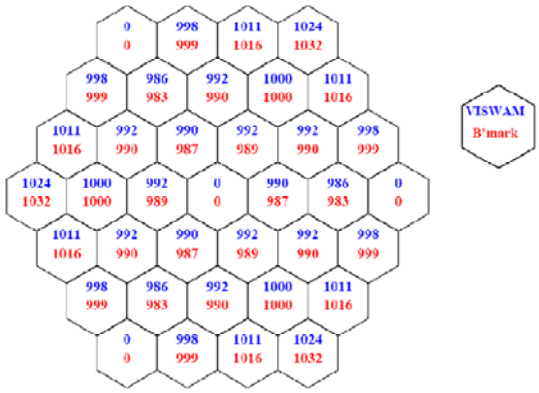

Fig. 8 - Comparison of Fission Density Distribution for 3.4%

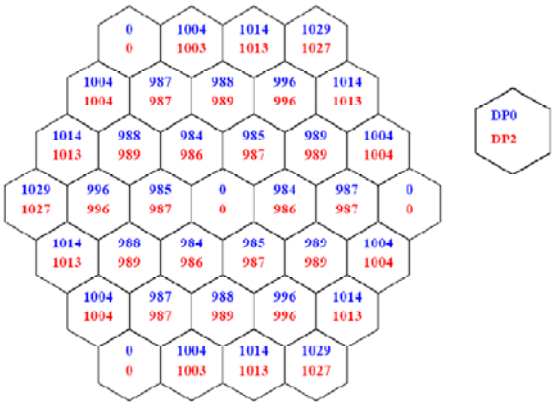

Fig. 9 - Fission Density Distribution for 4.8%

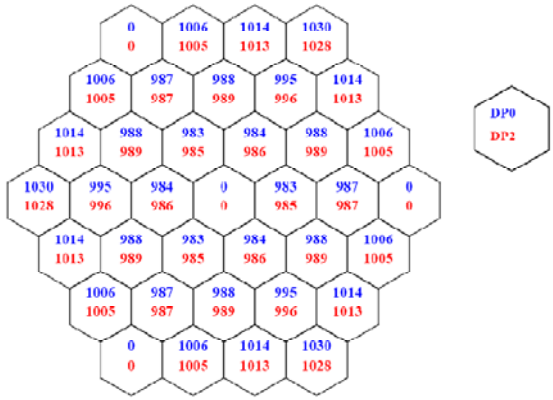

Fig. 10 - Fission Density Distribution for 5.2%

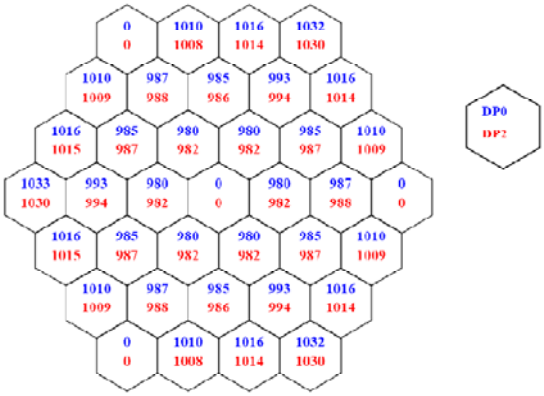

Fig. 11 - Fission Density Distribution for 6.3%

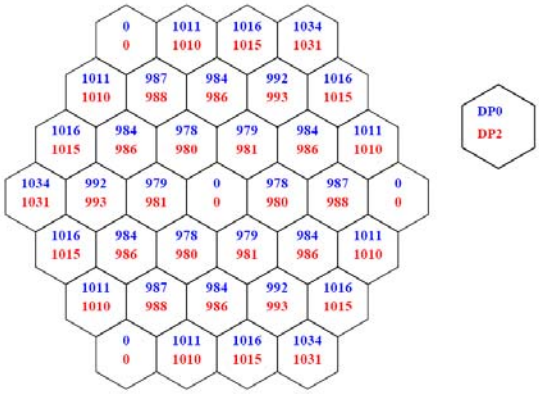

Fig. 12 - Fission Density Distribution for 6.7%

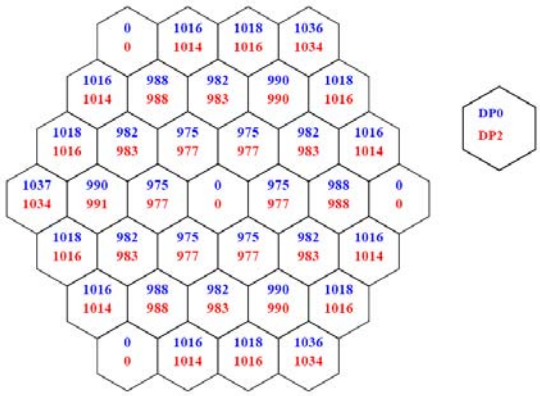

Fig. 13 - Fission Density Distribution for 7.9%

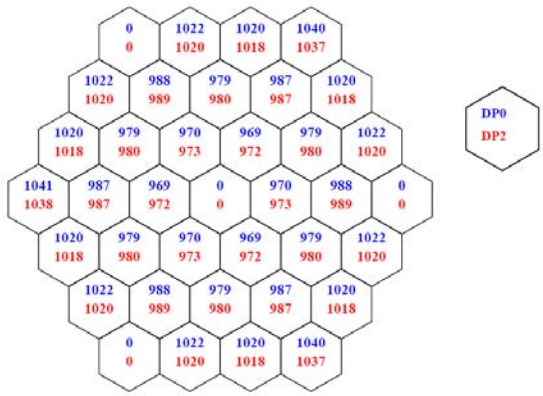

Fig. 14 - Fission Density Distribution for 9.9%

5. CONCLUSION

The lattice analysis codes in hexagonal geometry are needed because the reactor cores are being designed increasingly with triangular pitch. The 2D collision probability method has been applied to the high temperature test reactor benchmark problem in hexagonal geometry. In the assembly cell problem, the adjacent cells have been linked using interface currents. The incoming/outgoing angular flux at the pincell interface is expanded in P_N functions. The expansion is limited to P2. Reflective boundary condition is applied at the outermost surfaces. The results are compared for a single fuel pin and fuel assembly cell calculations. The results show a good agreement in k_∞ for pincell and assembly calculation (within 0.01% and 0.18%). The maximum difference in fission density distribution is 0.7% for the lowest enrichment. The P1 expansion in angular flux at region interface shows better matching in k_∞. In the current problem with graphite moderator there is no steep flux gradient within the fuel assembly as may be present in an assembly with light water as moderator. Therefore the use of P1 expansion is rather adequate to get the results within desirable accuracy. Use of higher order P2 expansion functions gives nearly same eigenvalue. It is planned to test the VISWAM code against other hexagonal assembly benchmark with strong heterogeneity like Gd cells and also as function of burnup. The CP method is seen to be a competitive option to other methods such as MOC, due to low running time and comparable accuracy.

6. ACKNOWLEDGEMENT

The authors are thankful to Shri K. N. Vyas, AD, RPG for encouraging the work. The first author is thankful to Dr. Usha Pal & Dr. R. Karthikeyan of LWRPS, RPDD for encouragement. The first author is also thankful to Shri Amod Kishore Mallick of RPDD for useful discussions.

7. REFERENCES

1. Suhail Ahmad Khan, Arvind Mathur, V. Jagannathan, L. Thilagam and D.K. Mohapatra, "Analysis of LEU pin cell Benchmark using VISWAM Code System", BARC Internal Report No. BARC/2013/I/010
2. Arvind Mathur, Suhail Ahmad Khan, V. Jagannathan, L. Thilagam and D.K. Mohapatra, "Validation of VISWAM Square Lattice Module with MOX pin cell Benchmark ", BARC Internal Report No. BARC/2013/I/009
3. Edenius M., Forssen B.H., Häggblom H., "Physics model development in CASMO", *In Int. Conf. Physics of Reactors: Operation, Design and Computation*, Marseille, France, P.IV-25 (1990).
4. Weiss Z.J., Stamm'ler R.J.J., "Nodal coupling of heterogeneous pin cells", *Trans. Am. Nucl. Soc*. **26**, 223 (1977).
5. Kavenoky A. and Sanchez R., "The APOLLO assembly spectrum code", *In Int. Topl. Mtg. Advances in Reactor Physics, Mathematics and Computation*, Paris, France, 1461 (1987).
6. Marleau G., Hérbert A., Roy R., *A User Guide for DRAGON Version 4*, Institut de génie nucléaire, Département de génie mécanique, École Polytechnique de Montréal (2011).
7. Sanchez, R., "A transport multicell method for two-dimensional lattices of hexagonal cells", *Nucl. Sci. Eng*. 92, 247. (1986)
8. Ouisloumen M, Marleau G., Hérbert A, Roy R., "Computation of Collision Probabilities for Mixed Hexagonal-Cylindrical Cells Using the DP1 Approximation to the $J_{\pm}$ technique", *Proc. Int. Topl. Mtg. Advances in Mathematics, Computations, and Reactor Physics*, Pittsburgh, PA, April 28 – May 02, 1991.
9. CARLVIK I. "A Method for Calculating Collision Probabilities in General Cylindrical Geometry and Applications to Flux Distributions and Dancoff Factors," *Proc. 3rd Int. Conf. Peaceful Uses of Atomic Energy,* Geneva, Switzerland, August 31-September 9, 1964, Vol. 2, p. 225, United Nations (1965).
10. Zhang Z., Rahnema F, Zhang D., Pounders J.M., Ougouag A.M., "Simplified two and three dimensional HTTR benchmark problems", *Ann. Nucl. Energy,* **38**, 1172 (2011).

11. Sanchez R. and McCormick N.J., “A Review of Neutron Transport Approximations”, *Nucl. Sci. Eng*, **80**, 481 (1982).

12. Sanchez R., “Approximate Solutions of the Two-Dimensional Integral Transport Equation by Collision Probability Methods”, *Nucl. Sci. Eng*, **64**, 384 (1977).

13. Marleau G, Dragon Theory Manual Part 1: Collision Probability Calculations, IGE-236 Rev. 1, (2001)

14. Marleau G, “DRAGON Theory for 3D CANDU Problems”, Atomic Energy of Canada Limited, April 20, 2004

15. Krishnani P D, “Analysis of 2-D LWR benchmarks with an interface current method for solving the integral transport equation”, *Ann. Nucl. Energy* , **14**, 463, (1987)

16. Villarino E.A., Stamm’ler R.J.J., Ferri A.A., Casal J.J., “HELIOS: angularly dependent collision probabilities” *Nucl. Sci. Eng*. **112**, 16–31 (1992).

17. Khan Suhail Ahmad & Mathur Arvind, “Transmission & Escape Probabilities for Double P2 expansion of Angular Flux”, RPDD/LWRPS/GEN/003/2015, June 05, 2015

18. Abramowitz M. and Stegun I.A., *Handbook of Mathematical Functions,* Dover Publications Inc, New York, (1972).

19. Lewis E.E. and Miller W. F. Jr., *Computational Methods of Neutron Transport*, John Wiley & Sons Inc, New York, (1984)

20. Yang Xue and Satvat Nader, “MOCUM: A two-dimensional method of characteristics code based on constructive solid geometry and unstructured meshing for general geometries”, *Ann. Nucl. Energy*, 46, 20, (2012)

Appendix A

Method of Ray Tracking

A large part of the computational effort in two dimensional collision probability calculations is incurred in the evaluation of the coefficient matrices of collision probabilities. The collision probability integrals in two dimensions depend on azimuthal angle and space variable *y*. These integrals are numerically evaluated by trapezoidal rule or other quadrature formula. This is normally known as ray tracing. For present study, we have adopted equidistant ray tracing method. In this method, parallel rays are drawn for each angle and their intersection with the hexagon or circular regions are found. The coordinate system used for ray tracing is shown in Fig. A-1. The origin is taken as the centre of hexagon or circle.

A.1 Definition of tracking line

For calculating tracks inside hexagon or circle, we need to find the intersection points with sides of hexagon and circles. The tracking line is uniquely defined by a point on the line and its slope. The

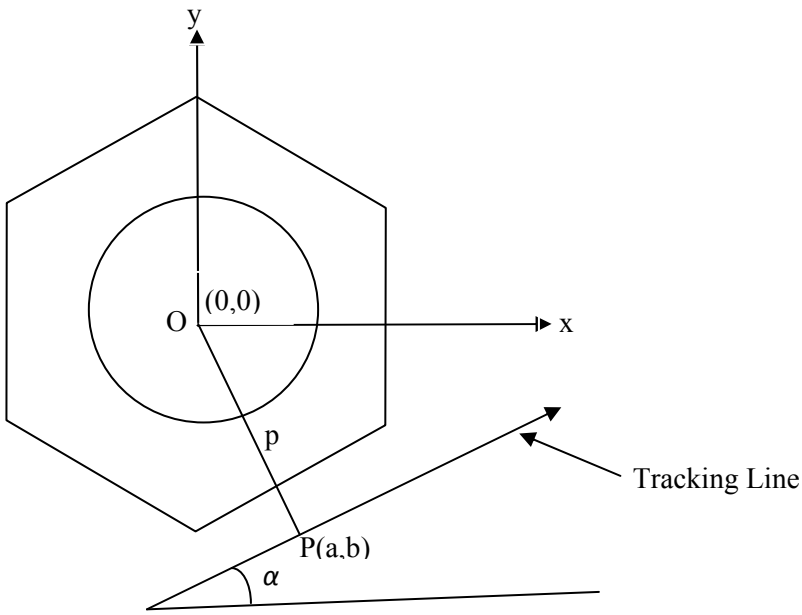

Fig. A-1 Definition of origin

tracking line is shown in the Figure A-1. Its slope is defined by $m_1 = \tan \alpha$. We have to define a point on this line to uniquely define it. For this a perpendicular OP is drawn on the tracking line from origin O.

If p is the length and (a, b) are the coordinates of the foot of perpendicular, then slope of perpendicular is given as

$$m_2 = -\frac{1}{m_1}$$

Equation of perpendicular $y = m_2 x + c$

Since it passes through origin O, so *c=0*. Point P also lies on this perpendicular line. So

$$b = m_2 a$$

Now, distance between points O & P is p. so

$$a^2 + b^2 = p^2$$

$$a^2 + a^2 m_2^2 = p^2$$

$$a = \frac{p}{\sqrt{(1 + m_2^2)}} = \frac{m_1 p}{\sqrt{(1 + m_1^2)}}$$

$$b = m_2 a = \frac{-p}{\sqrt{(1 + m_1^2)}}$$

The coordinates (a, b) and slope m_1 uniquely define the tracking line. The value of p is chosen initially as the side of hexagon for this hexagonal cell.

A.2 Intersection of tracking line with Circle

Once the tracking line is defined, its intersection points are computed with each circular region. A circle is uniquely defined by coordinates of its centre (*p, q*) and radius *r*. The equation of circle is given as

$$(x - p)^2 + (y - q)^2 = r^2$$

For a line passing through point (x_a, y_a) and slope *m* we first calculate

$$c = y_a - m x_a$$

then we calculate following quantities

$$A = 1 + m^2$$

$$B = 2m(c - q) - 2p$$

$$C = p^2 + (c - q)^2 - r^2$$

$$D = B^2 - 4AC$$

If $D > 0$, the line intersects the circle. The two points of intersection are given as

$$x_1 = \frac{-B + \sqrt{D}}{2A}; y_1 = m x_1 + c$$

$$x_2 = \frac{-B - \sqrt{D}}{2A}; y_2 = m x_2 + c$$

These points are stored and then sorted in increasing or decreasing order. If the tracking line is vertical (slope=∞) then considering equation of line *x=k*, we calculate

$$D = r^2 - (k - p)^2$$

If $D > 0$, the line intersects the circle. The two points of intersection are given as

$$x_1 = k \; ; y_1 = p + \sqrt{D}$$

$$x_2 = k \; ; y_2 = p - \sqrt{D}$$

After computing intersection points, the track length in a circle is computed as

$$t = \sqrt{(x_2 - x_1)^2 + (y_2 - y_1)^2}$$

A.3 Intersection of tracking line with Hexagon

The intersection of tracking line with hexagon involves the intersection of line with hexagonal surfaces. The surfaces of hexagon are numbered as shown in figure A-2. If the line crosses the hexagon, it will intersect any two surfaces defining the hexagon. The equations of surfaces of hexagon are stored and intersection with each surface checked at a time. Here we will describe to calculate the point of intersection of two lines.

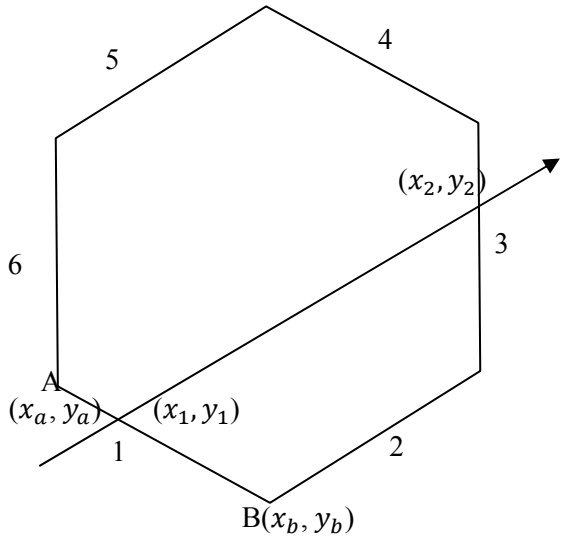

Fig. A-2 Surfaces of Hexagon

If $A_1x + B_1y = C_1$ and $A_2x + B_2y = C_2$ are the equations of two lines, then we calculate

$$D = A_1B_2 - A_2B_1$$

If $|D|$>0, the lines intersect and the point of intersection is give as

$$x = \frac{C_1B_2 - C_2B_1}{D} \; ; y = \frac{C_1A_2 - C_2A_1}{D}$$

The hexagon surface is defined by two vertices. For surface AB, as shown in fig. A-2, the slope of the surface can be obtained using

$$m_{AB} = \frac{y_b - y_a}{x_b - x_a}$$

The intercept on *y*-axis can be obtained

$$c_{AB} = y_b - m_{AB} x_b$$

Now the equation of line can be written as

$$y = m_{AB} x - c_{AB}$$

or rearranging

$$-m_{AB} x + y = -c_{AB}$$

Thus

$$A_1 = -m_{AB}, B_1 = 1, C_1 = -c_{AB}$$

Similarly for tracking line defined in section A.1, we have

$$A_2 = -m_1, B_2 = 1, C_2 = -c \;\; where \; c = b - m_1 a$$

The intersection point can be found using above formula. Once the intersection point is calculated, we have to check whether it lies on hexagon. For this purpose, we will compare (*x, y*) with the coordinates of the vertices of that surface. If the line intersects, say, surface AB (Fig. A-2), then point (*x,y*) will lie on hexagon if x lies between x_a & x_b and y lies between y_a & y_b. After checking the intersection with all six sides, we get two points of intersections denoted by (x_1, y_1) and (x_2, y_2) in Figure A-2. Now we want to know which surface of the hexagon is intersected first. For this purpose, we arrange both x_1 and x_2 intersection points in increasing order of their magnitude. With these points we have associated surface numbers 1 and 2. This order of their magnitude will give us the order and number of the surfaces encountered. The track length inside hexagon is again given by the formula

$$t = \sqrt{(x_2 - x_1)^2 + (y_2 - y_1)^2}$$

The above procedure is repeated for all angles and all parallel lines of an angle. The coordinates of intersection are stored for future calculation of optical length.

After tracking the full geometry, the volume of each zone is numerically computed. The formula for numerical volume is given by

$$V_i^{num} = \frac{1}{\alpha} \sum_m \sum_n w_A^m \, w_y^n \, t_i^{m,n}$$

where t_i is the track length in region *i* and α is the angle of integration. The ratio between true and numerically integrated volume is a measure of integration accuracy and serves as a numerical check for detecting any anomaly in ray tracing.

प्रकाशक :
Published by:
अध्यक्ष, वैज्ञानिक सूचना संसाधन प्रभाग
Head, Scientific Information Resource Division
भाभा परमाणु अनुसंधान केंद्र, ट्रॉम्बे, मुंबई - 400 085, भारत
Bhabha Atomic Research Centre, Trombay, Mumbai 400 085, India